

# *In Vitro* Characterization of a Stem-Cell-Seeded Triple-Interpenetrating-Network Hydrogel for Functional Regeneration of the Nucleus Pulposus

Lachlan J. Smith, PhD,<sup>1-3</sup> Deborah J. Gorth, MS,<sup>1-3</sup> Brent L. Showalter, BS,<sup>1,2,4</sup> Joseph A. Chiaro, BA,<sup>1-3</sup> Elizabeth E. Beattie, BS,<sup>2</sup> Dawn M. Elliott, PhD,<sup>4</sup> Robert L. Mauck, PhD,<sup>2,3</sup> Weiliam Chen, PhD,<sup>5</sup> and Neil R. Malhotra, MD<sup>1</sup>

Intervertebral disc degeneration is implicated as a major cause of low-back pain. There is a pressing need for new regenerative therapies for disc degeneration that restore native tissue structure and mechanical function. To that end we investigated the therapeutic potential of an injectable, triple-interpenetrating-network hydrogel comprised of dextran, chitosan, and teleostean, for functional regeneration of the nucleus pulposus (NP) of the intervertebral disc in a series of biomechanical, cytotoxicity, and tissue engineering studies. Biomechanical properties were evaluated as a function of gelation time, with the hydrogel reaching ~90% of steady-state aggregate modulus within 10 h. Hydrogel mechanical properties evaluated in confined and unconfined compression were comparable to native human NP properties. To confirm containment within the disc under physiological loading, toluidine-blue-labeled hydrogel was injected into human cadaveric spine segments after creation of a nucleotomy defect, and the segments were subjected to 10,000 cycles of loading. Gross analysis demonstrated no implant extrusion, and further, that the hydrogel interdigitated well with native NP. Constructs were next surface-seeded with NP cells and cultured for 14 days, confirming lack of hydrogel cytotoxicity, with the hydrogel maintaining NP cell viability and promoting proliferation. Next, to evaluate the potential of the hydrogel to support cell-mediated matrix production, constructs were seeded with mesenchymal stem cells (MSCs) and cultured under prochondrogenic conditions for up to 42 days. Importantly, the hydrogel maintained MSC viability and promoted proliferation, as evidenced by increasing DNA content with culture duration. MSCs differentiated along a chondrogenic lineage, evidenced by upregulation of aggrecan and collagen II mRNA, and increased GAG and collagen content, and mechanical properties with increasing culture duration. Collectively, these results establish the therapeutic potential of this novel hydrogel for functional regeneration of the NP. Future work will confirm the ability of this hydrogel to normalize the mechanical stability of cadaveric human motion segments, and advance the material toward human translation using preclinical large-animal models.

## Introduction

**L**OW-BACK PAIN is a prevalent, debilitating, and costly condition, with an economic impact exceeding \$90 billion annually in the United States and affecting up to 85% of the population.<sup>1,2</sup> Intervertebral disc degeneration is strongly implicated as a cause of low-back pain.<sup>3</sup> The intervertebral disc is a three-component structure comprised of a central, gelatinous nucleus pulposus (NP) and surrounding fibrocartilaginous annulus fibrosus situated between superior

and inferior cartilaginous endplates that interface with the vertebral bodies.<sup>4</sup> The primary function of the disc is mechanical. The proteoglycan-rich NP generates a swelling pressure that is constrained laterally by the annulus fibrosus and supports uniform transfer of compressive loads between the vertebral bodies, thus facilitating the complex motion of each intervertebral joint.<sup>5</sup> With increasing age discs begin to degenerate. Fundamental to disc degeneration is the progressive loss of proteoglycans and associated hydration from the NP. Dehydration compromises the ability of the NP to

Departments of <sup>1</sup>Neurosurgery and <sup>2</sup>Orthopedic Surgery, Perelman School of Medicine, University of Pennsylvania, Philadelphia, Pennsylvania.

<sup>3</sup>Translational Musculoskeletal Research Center, Philadelphia Veterans Affairs Medical Center, Philadelphia, Pennsylvania.

<sup>4</sup>Department of Biomedical Engineering, College of Engineering, University of Delaware, Newark, Delaware.

<sup>5</sup>Department of Surgery, New York University School of Medicine, New York, New York.

transfer and distribute compressive loads between the vertebrae, leading to loss of disc height and progressive structural and mechanical breakdown of the entire intervertebral joint.<sup>3,6</sup>

Current treatments for low-back pain resulting from disc degeneration are predominantly conservative.<sup>7</sup> Where surgical intervention is warranted, the current gold standard is spinal fusion,<sup>7</sup> wherein adjacent spinal segments are irrevocably joined together through induced bone growth. The goal with this approach is to alleviate painful symptoms, but it does not restore disc mechanics or structure. Recurrent episodes of pain are common, and adjacent levels of the spine may experience accelerated degeneration requiring additional surgery.<sup>8,9</sup> More recently, disc arthroplasty (artificial disc replacement) has been used to restore mobility; however, these implants do not recapitulate native nondegenerate mechanical function. Additionally, they are subjected to wear and failure, necessitating resection that is associated with risk of significant complications.<sup>8,9</sup> A key limitation of current treatments for disc degeneration is that they do not maintain or restore native tissue structure and mechanical function, and primarily address end-stage disease. Therefore, there is a strong need for new therapies to alter the course of disc degeneration and retain/restore disc structure and mechanical function by directly addressing the underlying causes and mechanisms.

To this end, hydrogel implants for treating disc degeneration have emerged as an area of active research, with the objective of augmenting native NP. Many promising biomaterials are being investigated, including hyaluronic acid composite hydrogels,<sup>10–15</sup> photo-crosslinked carboxymethylcellulose hydrogels,<sup>16,17</sup> and many others. It has been suggested that the ideal hydrogel for NP augmentation and repair would (1) be suitable for minimally invasive (percutaneous) delivery to the NP space, (2) solidify rapidly after implantation to avoid leakage of cells or gel, (3) be capable of restoring disc structure and function, (4) be biologically compatible with the existing NP cell population, and (5) support cell growth and matrix deposition by co-delivered cells, including native and stem cells.<sup>18</sup>

In this study we evaluated an *in situ* gelable, triple-interpenetrating-network hydrogel for functional regeneration of the NP. This hydrogel is comprised of three naturally derived materials: *N*-carboxyethyl chitosan, oxidized dextran, and teleostean.<sup>19</sup> Upon mixing, these components rapidly solidify at physiological temperatures in the absence of any extraneous crosslinking agents. Previous work has shown that the combination of these materials produces a hydrogel with increased resistance to biodegradation relative to single-network hydrogels, and improved mechanical strength as demonstrated by rheological characterization.<sup>19</sup> Previous work has also shown that *in vivo* subcutaneous injection of the hydrogel in mice does not induce a significant inflammatory response or evidence of tissue necrosis, suggesting that the hydrogel and its degradation by-products have minimal cytotoxicity concerns.<sup>19</sup>

The overall objective of this study was to investigate the potential of this hydrogel for NP regeneration. To achieve this, we first evaluated crosslinking kinetics and confirmed that the hydrogel attained steady-state mechanical properties within a clinically appropriate time frame. Second, we evaluated hydrogel mechanical properties in confined and

unconfined compression and compared them to those of native human NP tissue. Third, we investigated whether the hydrogel remained completely contained within the NPs of human spine segments subjected to prolonged, *ex vivo*, cyclic loading. Fourth, we investigated the cytocompatibility of the hydrogel with NP cells. Finally, we investigated whether the hydrogel supported survival and differentiation of, and functional biosynthesis by, mesenchymal stem cells (MSCs).

## Materials and Methods

### *Mechanical evaluation of crosslinking kinetics*

To fabricate the hydrogel, dextran, chitosan, and teleostean were purchased from Sigma Aldrich (St Louis, MO). Oxidized dextran and *N*-carboxyethyl chitosan were synthesized in the laboratory as described previously.<sup>16</sup> Aqueous solutions of 20% teleostean, 3% *N*-carboxyethyl chitosan, and 7.5% oxidized dextran were mixed at ratio of 1:1:2. The hydrogel was cast between two glass plates and constructs of 4-mm diameter  $\times$  2.25-mm thick were produced using a biopsy punch. Constructs were allowed to crosslink at 37°C for 24 h. To evaluate crosslinking kinetics, constructs were tested in confined compression at nine time points, ranging from 1 to 24 h following fabrication. Confined compression was performed according to previously described methods.<sup>20</sup> The testing system consisted of an acrylic chamber fixed above a porous, stainless steel platen within a testing bath filled with phosphate-buffered saline (PBS). Compression was applied using an impermeable ceramic indenter sized matched to the compression chamber, and attached to a mechanical testing system fitted with a 5-N load cell (Instron 5542, Norwood, MA). Samples were initially subjected to a 0.02-N preload held for 500 s, followed by a stress relaxation test. This consisted of 20% strain, calculated based on the sample thickness following preload, applied at a rate of 0.05%/s, followed by relaxation to equilibrium for 10 min. Aggregate modulus was calculated as the final, equilibrium stress (equilibrium force/sample area) divided by the applied strain.

### *Mechanical properties in comparison to native human NP*

Mechanical properties of the hydrogel (16 h after fabrication) were determined in both confined and unconfined compression (both  $n = 5$ ), and compared to native human NP tissue properties. Confined compression tests were performed on 4-mm diameter  $\times$  2.25-mm-thick hydrogel constructs using the protocol described previously. In addition to aggregate modulus, hydraulic permeability was calculated from the relaxation data using linear biphasic theory, assuming material isotropy.<sup>21</sup> Aggregate modulus and permeability were compared with human NP tissue samples ( $n = 3$ ) that were obtained from two intervertebral discs (Thompson grade 3),<sup>22</sup> obtained with IRB approval from the National Disease Research Interchange (Philadelphia, PA), which were tested in confined compression using an identical protocol. Human samples were produced using a 4-mm-diameter biopsy punch, and shaved to a uniform thickness of  $\sim$ 2.25 mm using a freezing-stage microtome. Hydrogel constructs were also tested in unconfined compression to determine Young's

modulus and Poisson's ratio. The testing system and loading protocol were similar to those previously published.<sup>23</sup> A custom-built, transparent, acrylate tank mounted on a 10-cm-tall platform was constructed and a digital camera (DMC TZ4; Panasonic, Osaka, Japan) was mounted directly underneath the testing surface. All samples were tested in a PBS bath. A flat, nonporous plunger was attached to the mechanical testing system fitted with a 5-N load cell. The plunger was lowered to make contact with the platform base to zero the instrument displacement. Hydrogel constructs were fabricated, as for confined compression, and stained with toluidine blue to improve delineation of sample boundaries. Each specimen was placed on the platform and a 0.02-N preload was applied for 500 s. An incremental stress-relaxation test was then performed consisting of five steps of 5% strain (at a rate of 0.05%/s), with each step followed by 600 s of relaxation. Prior and subsequent to each relaxation period, a digital image of the sample was manually acquired from below for lateral strain analysis. Images were acquired at 41 pixels/mm, and post-processed using ImageJ (NIH, Bethesda, MD). Specimen diameter was measured in triplicate for each image, and results were averaged to obtain the specimen diameter at the end of each relaxation period. Lateral strain  $\varepsilon_y$  was calculated as the ratio of change in specimen diameter to initial specimen diameter. Similarly, axial strain  $\varepsilon_x$  was computed as the ratio of change in cross-head displacement to initial cross-head height. Poisson's ratio was calculated as the slope of the resulting lateral versus axial strain curve according to the formula  $-\frac{\varepsilon_y}{\varepsilon_x}$ . Young's modulus was calculated for the final strain increment as the equilibrium stress (equilibrium force/sample area) divided by the applied strain. Poisson's ratio and Young's modulus were compared with previously published values from our laboratory for human NP tissue.<sup>23</sup>

#### *Hydrogel retention in human intervertebral discs subjected to cyclic loading*

Three human lumbar spines were obtained from institutionally approved sources (NDRI, Philadelphia, PA). L5/S1 vertebra-disc-vertebra spine motion segments were isolated and prepared for testing. Posterior bony elements and extraneous soft tissue were removed; 1.25-mm Kirschner wires were placed through the L5 and S1 vertebral bodies, which were potted in poly(methyl methacrylate). Nucleotomy was performed by creating a cruciate incision in the posterolateral annulus using a #11 scalpel blade, and 4-mm pituitary rongeurs were used to remove  $1.64 \pm 0.53$  g of nuclear material per sample ( $\sim 50\%$  of NP volume<sup>24</sup>). Hydrogel was fabricated as described, with toluidine blue stain (ThermoFisher Scientific, Waltham, MA) included to facilitate localization within the disc following testing. A 0.5-mL injection of hydrogel was made through the open cruciate incision. Motion segments were maintained at 37°C for 16 h in a PBS bath before undergoing cyclic loading using an electromechanical testing system (ElectroPuls E3000; Instron). The loading protocol consisted of 10,000 cycles of compression at 2 Hz between applied stresses of 0.12 and 0.96 MPa, which correspond to 0.25 and 2 times body weight for a disc of 1560 mm<sup>2</sup>.<sup>25</sup> During the loading protocol, motion segments were regularly observed for extrusion of hydrogel through annulotomy defect. After loading, discs were transected mid-axially, imaged, and macroscop-

ically examined for evidence of hydrogel extrusion and inter-digitation with the NP tissue.

#### *Hydrogel cytocompatibility and NP cell interactions*

NP cells were isolated from bovine caudal discs.<sup>20</sup> Briefly, NP tissue was excised from four intervertebral discs from each of eight bovine caudal spines purchased from a slaughterhouse according to institutional guidelines. This tissue was then incubated overnight at 37°C in high-glucose Dulbecco's modified Eagle's medium (DMEM) containing 2% penicillin/streptomycin/fugizone (PSF). Tissue was digested using a two-step enzyme protocol consisting of 1 h in 2.5 mg/mL pronase (Merck, Darmstadt, Germany) followed by 4 h in 0.5 mg/mL collagenase (Type IV; Sigma Aldrich). NP cells were filtered through a 70- $\mu$ m strainer before being counted and resuspended at a density of 400,000 cells/mL in basal media (DMEM containing 1% PSF and 10% fetal bovine serum). A 15- $\mu$ L aliquot of this cell suspension was seeded onto prepolymerized hydrogel constructs. Seeded constructs were then cultured for 14 days in basal media, with media changes performed every 3 days. Constructs ( $n=3$ ) were harvested for qualitative assessment of cell viability and infiltration using live-dead staining (Life Technologies, Carlsbad, CA), with the construct surface imaged using fluorescence microscopy (Eclipse TE2000U; Nikon, Tokyo, Japan). For assessment of cell infiltration, harvested constructs ( $n=3$ ) were fixed in 4% paraformaldehyde and processed for paraffin histology. Sections were stained with 4',6-diamidino-2-phenylindole (DAPI), and observed and imaged using fluorescence microscopy (Eclipse 90i; Nikon).

#### *MSC survival, differentiation, and functional maturation*

To further assess the translational potential of the hydrogel, bovine MSCs were isolated as previously described<sup>26</sup> and directly encapsulated. Briefly, cells were obtained from the femurs or tibiae of two freshly slaughtered 3–6-month-old calves (Research 87, Boylston, MA).<sup>27</sup> Marrow was flushed into 5 mL of DMEM with 1% PSF and 300 U/mL heparin, centrifuged, and plated. The resulting MSCs were expanded to passage 2 before being suspended in 3% *N*-carboxyethyl chitosan such that the final seeding density following combination of the three hydrogel components was  $20 \times 10^6$ /mL. Cell-seeded, hydrogel constructs were fabricated as described and then cultured for 0, 14, or 42 days in a chemically defined media with (CM<sup>+</sup>) or without (CM<sup>-</sup>) 10 ng/mL TGF- $\beta$ 3 (R&D Systems, Minneapolis, MN), in a standard 5% CO<sub>2</sub> incubator. The complete media formulation has been published previously.<sup>20</sup>

Constructs ( $n=3$ ) cultured for 42 days in CM<sup>+</sup> were qualitatively examined for cell viability using live-dead staining. Constructs ( $n=5$ ) cultured for 0, 14, or 42 days in CM<sup>+</sup> and CM<sup>-</sup> were tested in unconfined compression testing as described previously, and Young's modulus was determined. These same constructs were then digested overnight in papain at 60°C. Sulfated glycosaminoglycan content ( $n=5$ ) was determined using the dimethylmethylene blue assay,<sup>28</sup> and reported as GAG/construct. DNA content was determined using the PicoGreen assay (Life Technologies, Grand Island, NY), and is reported as DNA/construct.

For histological analysis of extracellular matrix deposition, constructs ( $n=3$ ) from each time point and culture

condition were processed into paraffin and sections were immunostained for collagen II and chondroitin sulfate using bovine-specific antibodies (Sigma Aldrich). Following rehydration, the following incubation steps were performed: hyaluronidase (300 mg/mL; Sigma Aldrich) for 60 min at room temperature (RT), 3% hydrogen peroxide for 15 min at RT, proteinase K (Dako, Glostrup, Denmark) for 4 min at RT, peptide blocking agent (Background Buster; Innovex Biosciences, Richmond, CA) for 30 min at RT, and primary antibody overnight (both 1:200 dilution) at 4°C. Secondary detection was performed using an HRP polymer conjugate and visualized using 3,3'-diaminobenzidine (SuperPicture; Life Technologies). Stained sections were observed and imaged using light microscopy (Eclipse 90i; Nikon).

Messenger RNA analysis was performed for constructs ( $n=3$ ) for each time point and culture condition. RNA was isolated using a TRIZOL-chloroform extraction, and spectrophotometrically quantified (ND-1000; Nanodrop Technologies, Wilmington, DE). Reverse transcription was performed on 1  $\mu$ g of RNA in a 20- $\mu$ L volume (Superscript II; Life Technologies). mRNA expression levels of aggrecan, collagen II, and *SOX9* were determined by quantitative real-time PCR (StepOne Plus; Applied Biosystems, Carlsbad, CA). Expression levels were calculated using the comparative cycle threshold method and normalized to *GAPDH*.<sup>29</sup> Primer sequences for all genes were published previously.<sup>20</sup>

Results are presented as mean  $\pm$  standard deviation. Effects of culture time and media condition on measured properties (Young's modulus, GAG and DNA contents, and mRNA expression) were determined using two-way ANOVAs. Where a significant effect of either factor was detected, *post hoc* pairwise tests were performed. Significance was defined as  $p < 0.05$ .

## Results

### Mechanical evaluation of crosslinking kinetics

To evaluate the crosslinking kinetics of the hydrogel, mechanical properties were measured in confined compression at regular intervals over the course of 24 h. Aggregate modulus increased logarithmically with time

( $r^2=0.96$ , Fig. 1A), reaching 90% of its steady state value after 10 h.

### Hydrogel mechanical properties in comparison to human NP

Mechanical properties of hydrogel constructs were measured after 16 h of crosslinking in confined and unconfined compression, and compared to human NP properties (Fig. 1B). Hydrogel aggregate modulus was 30% of that of human NP ( $p < 0.05$ ). Hydrogel permeability, Young's modulus, and Poisson's ratio were not significantly different from those of human NP (Fig. 1B<sup>23</sup>).

### Hydrogel retention in human intervertebral discs subjected to cyclic loading

Delivery of hydrogel to the disc via a 19-gauge needle is illustrated in Figure 2A. No extrusion of toluidine-blue-stained hydrogel was observed during 10,000 cycles of physiologic loading. Similarly, macroscopic examination of axially bisected discs revealed no evidence of extrusion through the annular defect used to create the nucleotomy. Further, these gross images revealed that the hydrogel was closely inter-digitated with the surrounding native NP tissue (Fig. 2B).

### Hydrogel cytocompatibility and NP cell interactions

Qualitative analysis of live-dead staining indicated that the majority of cells remained viable (green fluorescence) after 2 weeks of culture on the hydrogel surface and there was evidence of colony formation and proliferation (Fig. 3A). Cross-sectional images of DAPI-stained sections demonstrated adherence of cells to the hydrogel surface; however, there was minimal cellular infiltration at this time point, indicative of the stable nature of the hydrogel (Fig. 3B).

### MSC survival, differentiation, and functional maturation

Qualitative analysis of live-dead staining indicated that the majority of MSCs remained viable (green fluorescence) after 42 days of culture in the hydrogel (Fig. 4A). For constructs cultured in CM<sup>-</sup>, DNA content was 85% and

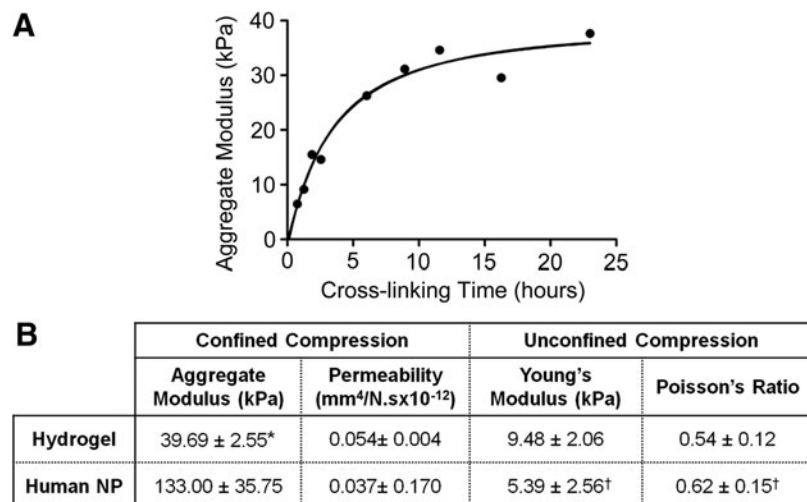


**FIG. 1.** (A) Mechanical evaluation of hydrogel crosslinking kinetics. Aggregate modulus from confined compression tests demonstrates that the hydrogel attained 90% of ultimate mechanical properties after  $\sim 10$  h. Solid line represents a logarithmic curve fit ( $r^2=0.96$ ). (B) Mechanical properties of hydrogel constructs in comparison to native human nucleus pulposus (NP). \* $p < 0.05$  versus human; † values from Cloyd *et al.*<sup>23</sup>

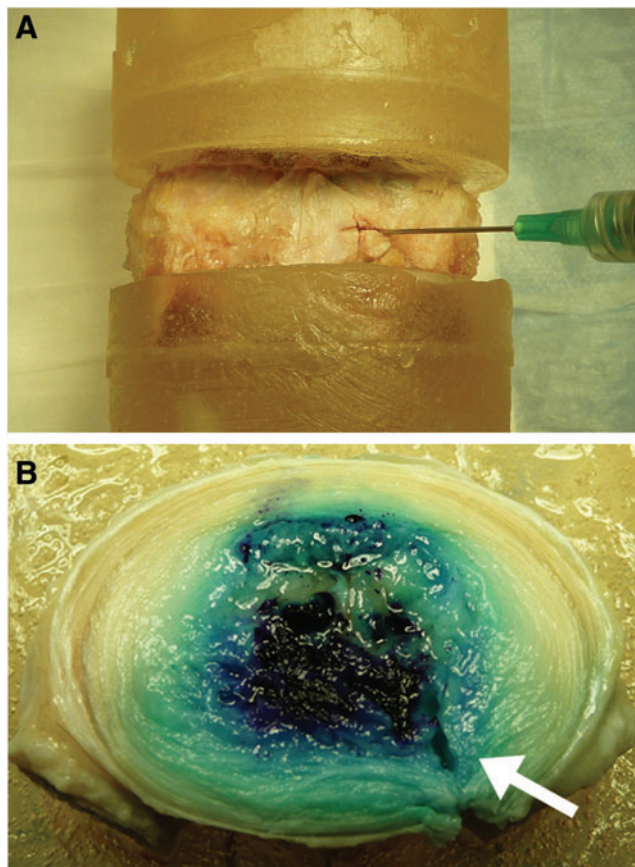


**FIG. 2.** (A) Injection of the hydrogel into the NP of an L5-S1 human intervertebral disc using a 19-gauge needle, following creation of a nucleotomy defect. (B) Macroscopic evaluation of an axially bisected disc following 10,000 cycles of loading in axial compression at 2 Hz between applied stresses of 0.12 and 0.96 MPa, which correspond to 0.25 and 2 times body weight. No evidence of hydrogel (blue) extrusion was observed through the annular defect (arrow) used to create the nucleotomy, and the hydrogel appeared well-integrated with the native tissue. Color images available online at [www.liebertpub.com/tea](http://www.liebertpub.com/tea)

88% of day 0 after 14 and 42 days of culture, respectively (with neither significantly different from day 0, Fig. 4B). For constructs cultured in  $CM^+$ , DNA content was 1.4- and 2.1-fold greater after 14 and 42 days of culture, respectively, compared with day 0 ( $p < 0.05$  for 42 days only). DNA content was significantly greater for constructs cultured in

$CM^+$  compared with  $CM^-$  after 42 days, but not after 14 days of culture.

With respect to composition, immunohistochemical analysis revealed progressive deposition of collagen II and chondroitin sulfate for constructs cultured in  $CM^+$ , with minimal deposition for constructs cultured in  $CM^-$  (Fig. 5A). For constructs cultured in  $CM^-$ , GAG content was 1.2- and 1.1-fold greater after 14 and 42 days of culture, respectively, compared with day 0 (neither significantly different, Fig. 5B). For constructs cultured in  $CM^+$ , GAG content was 1.8- and 2.3-fold greater after 14 and 42 days of culture, respectively, compared with day 0 ( $p < 0.05$  for 42 days only). GAG content was significantly greater for constructs cultured in  $CM^+$  compared with  $CM^-$  after 42 days, but not after 14 days of culture.

With respect to mechanical properties, for MSC-seeded constructs cultured in  $CM^-$ , Young's modulus was 2.7- and 2.6-fold greater after 14 and 42 days of culture, respectively, compared with day 0 ( $p < 0.05$  for both, Fig. 5C). For constructs cultured in  $CM^+$ , Young's modulus was 4.4- and 8.6-fold greater after 14 and 42 days of culture, respectively, compared with day 0 ( $p < 0.05$  for both). At both 14 and 42 days, Young's modulus was significantly greater for constructs cultured in  $CM^+$  compared with those cultured in  $CM^-$  conditions.

Finally, with respect to mRNA expression, for constructs cultured in  $CM^-$ , aggrecan expression was 4.3- and 37-fold greater after 14 and 42 days of culture, respectively, compared with day 0 (neither significantly different, Fig. 6A). For constructs cultured in  $CM^+$ , aggrecan expression was 17- and 69-fold greater after 14 and 42 days of culture, respectively, compared with day 0 ( $p < 0.05$  at 42 days only). After 42 days of culture, aggrecan expression was significantly greater for constructs cultured in  $CM^+$  compared with those cultured in  $CM^-$ , but not after 14 days of culture. For constructs cultured in  $CM^-$ , collagen II expression was 1.2- and 17-fold greater after 14 and 42 days of culture, respectively, compared with day 0 (neither significantly different, Fig. 6B). For constructs cultured in  $CM^+$ , collagen II expression was 78- and 72-fold greater after 14 and 42 days of culture, respectively, compared with day 0 (neither significantly different). After 14 days of culture, collagen II expression was significantly greater for constructs cultured in  $CM^+$  compared with those cultured in  $CM^-$ , but not after 42 days. For constructs cultured in  $CM^-$ , *SOX9* expression was 3.3- and 1.3-fold greater after 14 and 42 days of culture, respectively, compared with day 0 (neither significantly different, Fig. 6C). For constructs

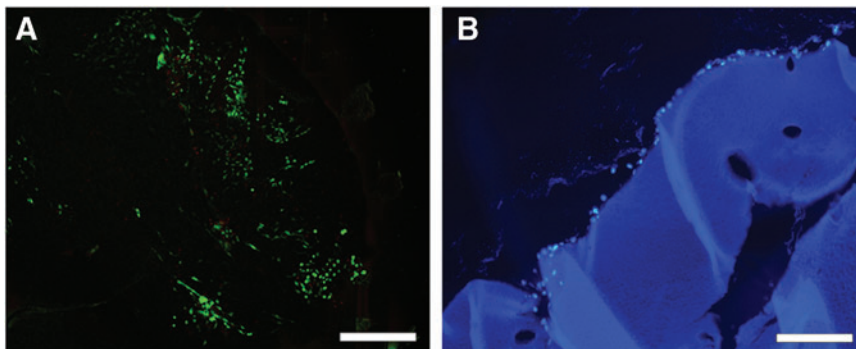
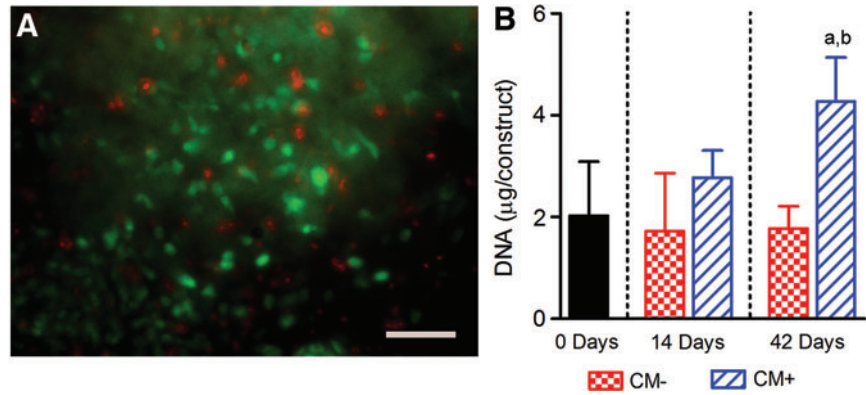


**FIG. 3.** (A) Live-dead stain demonstrates that viable bovine NP cells adhered to and proliferated on the surface of the hydrogel after 14 days of *in vitro* culture. (B) 4',6-Diamidino-2-phenylindole (DAPI) staining of hydrogel cross-section showing NP cell surface adherence but minimal infiltration. Scale bars = 200  $\mu$ m. Color images available online at [www.liebertpub.com/tea](http://www.liebertpub.com/tea)

**FIG. 4.** (A) Live-dead stain of a mesenchymal stem cell (MSC)-seeded hydrogel construct cross-section demonstrating viability after 42 days of *in vitro* culture in CM<sup>+</sup>. Scale bar = 100  $\mu$ m. (B) Differences in MSC-seeded hydrogel construct DNA content with culture time and media condition. Results are presented as mean  $\pm$  SD; <sup>a</sup> $p < 0.05$  versus 0 days; <sup>b</sup> $p < 0.05$  versus CM<sup>-</sup>. Color images available online at [www.liebertpub.com/tea](http://www.liebertpub.com/tea)



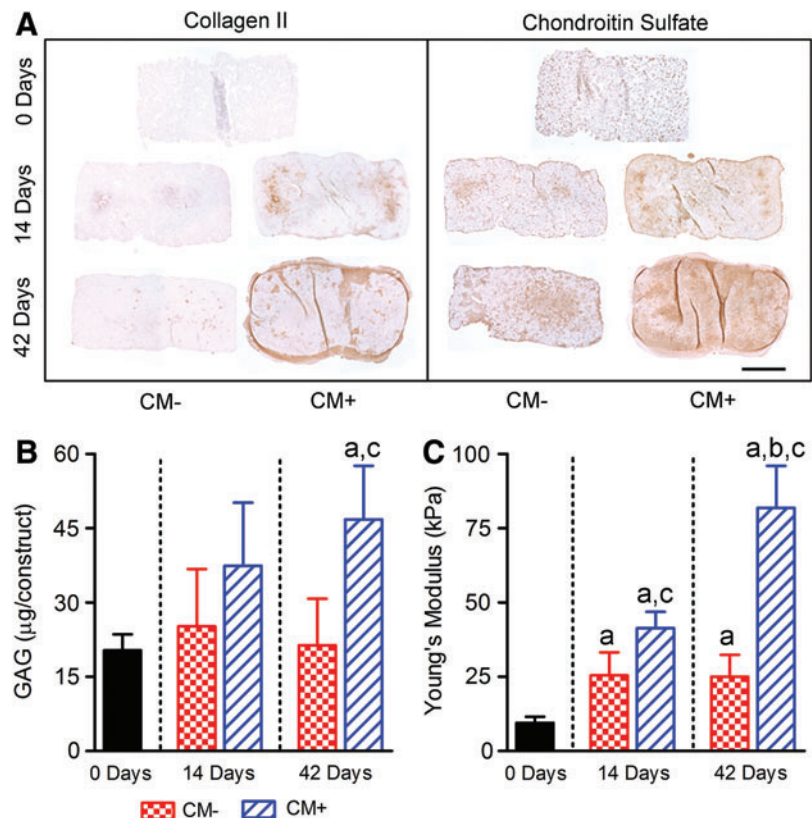
cultured in CM<sup>+</sup>, *SOX9* expression was fourfold greater than day 0 after 14 days of culture, but 96% of day 0 after 42 days of culture (neither significantly different). After both 14 and 42 days of culture, *SOX9* expression was not significantly different for constructs cultured in CM<sup>+</sup> compared with those cultured in CM<sup>-</sup> conditions.

### Discussion

The objective of this study was to evaluate the potential of a novel *in situ* gelable triple-interpenetrating-network hydrogel for functional regeneration of the NP. Advantages of this hydrogel include its suitability for injectable delivery, the fact that it solidifies without the aid of extraneous crosslinking agents, and that it is composed of naturally derived materials.<sup>19</sup> The three-component hydrogel described here self-assembles primarily via Schiff bases and

ionic bond formation.<sup>19,30,31</sup> All materials (dextran, chitosan, and teleostean) are naturally derived; the dextran and chitosan are minimally modified. The selected formulation was designed to make clinical application feasible. The combined solution is a liquid at RT prior to gelation, a critical factor when considering injectable delivery. Teleostean in solution remains a liquid until the temperature drops to below 8°C, thus facilitating material preparation. While the chitosan and dextran alone will form a hydrogel, its mechanical strength is relatively low as an implant. Increasing the concentrations of both chitosan and dextran can greatly enhance the hydrogel strength, but it also greatly accelerates the gelation process rendering these high-concentration formulations not practical for translational treatment paradigms. Adding teleostean enhances mechanical strength (by forming extra hydrogel networks and increasing material mass) while not accelerating the gelation time.<sup>19</sup>

**FIG. 5.** Effects of culture time and media condition on the composition and mechanical properties of MSC-seeded hydrogel constructs. (A) Representative immunohistological staining for collagen II and chondroitin sulfate; scale bar = 1 mm. (B) Sulfated GAG content and (C) Young's modulus from unconfined compression tests (both  $n = 5$ ). Results are presented as mean  $\pm$  SD; <sup>a</sup> $p < 0.05$  versus 0 days; <sup>b</sup> $p < 0.05$  versus 14 days; <sup>c</sup> $p < 0.05$  versus CM<sup>-</sup>. Color images available online at [www.liebertpub.com/tea](http://www.liebertpub.com/tea)



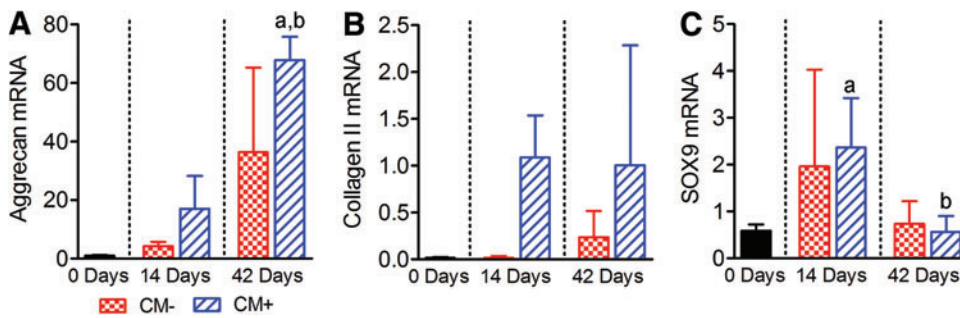


**FIG. 6.** Effects of culture time and media condition on mRNA expression levels (% GAPDH) for MSC-seeded hydrogel constructs ( $n = 3$ ). (A) Aggrecan. (B) Collagen II. (C) SOX9. Results are presented as mean  $\pm$  SD; <sup>a</sup> $p < 0.05$  versus 0 days; <sup>b</sup> $p < 0.05$  versus 14 days. Color images available online at [www.liebertpub.com/tea](http://www.liebertpub.com/tea)

A critical benchmark for the success of NP implants in the clinical context is that they remain contained within the disc space. Implant extrusion may lead to spinal cord or nerve root compression, which may be associated with serious neurological complications. A large number of NP implant materials have been investigated in recent years,<sup>32,33</sup> spanning the spectrum from injectable, viscous polymers, to solid, structural implants. A small number of these implants have progressed to clinical trials with mixed results.<sup>32</sup> While few long-term studies have been conducted, it is likely that solid structural implants would be subjected to wear and potential failure, as has been found for total-disc replacements.<sup>9</sup> Further, solid implants necessitate invasive delivery that is associated with structural damage. The injectable hydrogel evaluated in the present study remained within the disc space following extensive *in vitro* cyclic loading, despite the presence of a large annular defect resulting from creation of the nucleotomy. The hydrogel also appeared well-integrated with native tissue structures upon macroscopic examination (Fig. 2B).

Mechanical properties of the acellular hydrogel compared favorably with native tissue properties, and while acellular hydrogel implants may be able to restore some level of disc function (i.e., height), they suffer from the same limitation as other material implants in that they will undergo progressive degradation, potentially limiting their long-term therapeutic efficacy. Previous work has demonstrated that this hydrogel has a degradation half-life of around 6 weeks *in vivo*.<sup>19</sup> Ideally, as the implant degrades it would be replaced by *de novo* extracellular matrix. Due to the low cell density present in the NP,<sup>34</sup> however, the capacity of endogenous cells to form new tissue formation is limited. One option for overcoming this limitation is to codeliver an exogenous cell type, such as MSCs with the hydrogel. Codelivered MSCs have the potential to replace the hydrogel material as it degrades with newly formed tissue. A major advantage of using MSCs is that they can be harvested with minimal donor site morbidity, expanded *in vitro*, and reimplanted autologously. Additionally, studies have shown that with appropriate biochemical cues, it is possible to direct MSCs toward an NP-cell-like phenotype.<sup>35</sup> In this study we investigated the capacity of the hydrogel to act as a delivery vehicle for MSCs, and as a scaffold for functional biosynthesis. Importantly, the hydrogel maintained long-term viability of MSCs and promoted their proliferation, as evidenced by increased DNA content. Additionally, MSCs differentiated along a chondrogenic lineage, as evidenced by upregulation of aggrecan and collagen II. Interestingly, while levels of both genes were higher in the presence of

TGF- $\beta$ 3, cells in the gel alone showed substantial upregulation of these genes, perhaps indicative of a prochondrogenic effect of the gel alone. Consistent with previous studies, we noted a transient upregulation of SOX9 at 14 days. This chondrogenic transcription factor is often upregulated during early MSC commitment to the lineage, and then downregulated thereafter.

Biosynthetic activity of MSCs in the presence of TGF- $\beta$ 3 was also evidenced by increasing GAG, collagen, and mechanical properties with increasing culture time. Mechanical properties for MSCs cultured in this hydrogel achieved after 42 days of culture compare favorably with those reported previously for MSCs cultured in other hydrogels with the same seeding density and media conditions, including methacrylated hyaluronic acid and Puramatrix (approximately fourfold and threefold greater Young's modulus, respectively), although somewhat less than for agarose ( $\sim 50\%$  lower Young's modulus).<sup>36</sup>

We have previously demonstrated that an injectable hydrogel, similar to the one evaluated in the current study, is capable of normalizing disc mechanical properties following creation of a nucleotomy defect<sup>37</sup>; however, it is unlikely that this or any other injectable NP implant would be capable of permanently restoring the structure and biomechanical function of a severely degenerated disc. We anticipate that an appropriate clinical target population for injectable hydrogels, such as the one evaluated here, would be those individuals with intermediate-stage, symptomatic disc degeneration. Indeed, of the 15 million patients that primary care physicians see per year for low-back pain, only 500,000 will have severe, late-stage, degeneration and meet criteria for surgery.<sup>38</sup> However, four million patients who do not meet surgical criteria have moderate disc degeneration, and are unresponsive to conservative treatments, such as steroid injections and physical therapy. There is therefore a very strong unmet need for novel therapeutic strategies to treat disc degeneration in these patients. For individuals with late-stage disc degeneration, surgical interventions are likely to remain more effective options. In the future, biological, tissue-engineered total-disc replacements such as those currently under development<sup>39,40</sup> may also present a viable therapeutic option for these patients.

A limitation of the cell culture studies presented here was that they were conducted under "idealized" biochemical conditions that are conducive to MSC survival and function. The *in vivo* biochemical microenvironment of the NP, which is characterized by poor nutrition, low oxygen, and low pH, represents a challenge for MSC-based therapies, as there is evidence that these cells are particularly sensitive to

microenvironmental stress.<sup>41–43</sup> Future work will establish how these environmental factors mediate MSC viability and biosynthetic potential, and explore ways to condition MSCs to maximize their regenerative potential upon delivery to the *in vivo* space. An additional challenge faced when delivering MSC-based therapies to the degenerate disc is the presence of chronic inflammation<sup>44</sup>; there is evidence that inflammation may limit the regenerative potential of MSCs.<sup>45</sup> To address this challenge, we have previously developed sustained-release anti-inflammatory therapeutics that can be delivered locally to the disc space.<sup>46</sup> Ongoing studies seek to integrate this anti-inflammatory component with the MSC-seeded injectable hydrogel described here, in order to provide a microenvironment that is overall more conducive to regeneration.

In summary, in this series of *in vitro* studies, we have established the potential of this novel hydrogel for long-term functional regeneration of the NP. In ongoing studies we are investigating the long-term biomechanical stability of the hydrogel implant, initially in cadaveric human spine segments, and subsequently *in vivo*, in a large-animal model of disc degeneration.

#### Acknowledgments

This project was funded by grants from the Neurosurgery Research and Education Foundation and the Department of Veterans Affairs (IO1RX000211), and was supported by the Histology and Biomechanics cores of the Penn Center for Musculoskeletal Disorders (NIH P30 AR050950).

#### Disclosure Statement

The authors have no competing financial interests to disclose.

#### References

- Andersson, G.B. Epidemiological features of chronic low-back pain. *Lancet* **354**, 581, 1999.
- Katz, J.N. Lumbar disc disorders and low-back pain: socioeconomic factors and consequences. *J Bone Joint Surg Am* **88(Suppl 2)**, 21, 2006.
- Freemont, A.J. The cellular pathobiology of the degenerate intervertebral disc and discogenic back pain. *Rheumatology* **48**, 5, 2009.
- Humzah, M.D., and Soames, R.W. Human intervertebral disc: structure and function. *Anat Rec* **220**, 337, 1988.
- Schmidt, H., Kettler, A., Heuer, F., Simon, U., Claes, L., and Wilke, H.J. Intradiscal pressure, shear strain, and fiber strain in the intervertebral disc under combined loading. *Spine* **32**, 748, 2007.
- Urban, J.P., and Roberts, S. Degeneration of the intervertebral disc. *Arthritis Res Ther* **5**, 120, 2003.
- Mirza, S.K., and Deyo, R.A. Systematic review of randomized trials comparing lumbar fusion surgery to non-operative care for treatment of chronic back pain. *Spine* **32**, 816, 2007.
- Ghiselli, G., Wang, J.C., Bhatia, N.N., Hsu, W.K., and Dawson, E.G. Adjacent segment degeneration in the lumbar spine. *J Bone Joint Surg Am* **86-A**, 1497, 2004.
- Hanley, E.N., Jr., Herkowitz, H.N., Kirkpatrick, J.S., Wang, J.C., Chen, M.N., and Kang, J.D. Debating the value of spine surgery. *J Bone Joint Surg Am* **92**, 1293, 2010.
- Calderon, L., Collin, E., Velasco-Bayon, D., Murphy, M., O'Halloran, D., and Pandit, A. Type II collagen-hyaluronan hydrogel—a step towards a scaffold for intervertebral disc tissue engineering. *Eur Cell Mater* **20**, 134, 2010.
- Chen, Y.C., Su, W.Y., Yang, S.H., Gefen, A., and Lin, F.H. *In situ* forming hydrogels composed of oxidized high molecular weight hyaluronic acid and gelatin for nucleus pulposus regeneration. *Acta Biomater* **9**, 5181, 2013.
- Moss, I.L., Gordon, L., Woodhouse, K.A., Whyne, C.M., and Yee, A.J. A novel thiol-modified hyaluronan and elastin-like polypeptide composite material for tissue engineering of the nucleus pulposus of the intervertebral disc. *Spine (Phila Pa 1976)* **36**, 1022, 2011.
- Collin, E.C., Grad, S., Zeugolis, D.I., Vinatier, C.S., Clouet, J.R., Guicheux, J.J., *et al.* An injectable vehicle for nucleus pulposus cell-based therapy. *Biomaterials* **32**, 2862, 2011.
- Peroglio, M., Eglin, D., Benneker, L.M., Alini, M., and Grad, S. Thermoreversible hyaluronan-based hydrogel supports *in vitro* and *ex vivo* disc-like differentiation of human mesenchymal stem cells. *Spine J* **13**, 1627, 2013.
- Peroglio, M., Grad, S., Mortisen, D., Sprecher, C.M., Illien-Junger, S., Alini, M., *et al.* Injectable thermoreversible hyaluronan-based hydrogels for nucleus pulposus cell encapsulation. *Eur Spine J* **21(Suppl 6)**, S839, 2012.
- Gupta, M.S., Cooper, E.S., and Nicoll, S.B. Transforming growth factor-beta 3 stimulates cartilage matrix elaboration by human marrow-derived stromal cells encapsulated in photocrosslinked carboxymethylcellulose hydrogels: potential for nucleus pulposus replacement. *Tissue Eng Part A* **17**, 2903, 2011.
- Reza, A.T., and Nicoll, S.B. Characterization of novel photocrosslinked carboxymethylcellulose hydrogels for encapsulation of nucleus pulposus cells. *Acta Biomaterialia* **6**, 179, 2010.
- Chan, S.C., and Gantenbein-Ritter, B. Intervertebral disc regeneration or repair with biomaterials and stem cell therapy—feasible or fiction? *Swiss Med Wkly* **142**, w13598, 2012.
- Zhang, H., Qadeer, A., Mynarcik, D., and Chen, W. Delivery of rosiglitazone from an injectable triple interpenetrating network hydrogel composed of naturally derived materials. *Biomaterials* **32**, 890, 2011.
- Smith, L.J., Chiaro, J.A., Nerurkar, N.L., Cortes, D.H., Horava, S.D., Hebel, N.M., *et al.* Nucleus pulposus cells synthesize a functional extracellular matrix and respond to inflammatory cytokine treatment following long term agarose culture. *Eur Cell Mater* **22**, 291, 2011.
- Soltz, M.A., and Ateshian, G.A. Experimental verification and theoretical prediction of cartilage interstitial fluid pressurization at an impermeable contact interface in confined compression. *J Biomech* **31**, 927, 1998.
- Thompson, J.P., Pearce, R.H., Schechter, M.T., Adams, M.E., Tsang, I.K., and Bishop, P.B. Preliminary evaluation of a scheme for grading the gross morphology of the human intervertebral disc. *Spine* **15**, 411, 1990.
- Cloyd, J.M., Malhotra, N.R., Weng, L., Chen, W., Mauck, R.L., and Elliott, D.M. Material properties in unconfined compression of human nucleus pulposus, injectable hyaluronic acid-based hydrogels and tissue engineering scaffolds. *Eur Spine J* **16**, 1892, 2007.
- Dullerud, R., Amundsen, T., Johansen, J.G., and Magnaes, B. Lumbar percutaneous automated nucleotomy. Technique, patient selection and preliminary results. *Acta Radiol* **34**, 536, 1993.



25. Beckstein, J.C., Sen, S., Schaer, T.P., Vresilovic, E.J., and Elliott, D.M. Comparison of animal discs used in disc research to human lumbar disc: axial compression mechanics and glycosaminoglycan content. *Spine (Phila Pa 1976)* **33**, E166, 2008.
26. Mauck, R.L., Yuan, X., and Tuan, R.S. Chondrogenic differentiation and functional maturation of bovine mesenchymal stem cells in long-term agarose culture. *Osteoarthritis Cartilage* **14**, 179, 2006.
27. Huang, A.H., Yeger-McKeever, M., Stein, A., and Mauck, R.L. Tensile properties of engineered cartilage formed from chondrocyte- and MSC-laden hydrogels. *Osteoarthritis Cartilage* **16**, 1074, 2008.
28. Farndale, R.W., Sayers, C.A., and Barrett, A.J. A direct spectrophotometric microassay for sulfated glycosaminoglycans in cartilage cultures. *Connect Tissue Res* **9**, 247, 1982.
29. Schmittgen, T.D., and Livak, K.J. Analyzing real-time PCR data by the comparative C(T) method. *Nat Protoc* **3**, 1101, 2008.
30. Weng, L., Romanov, A., Rooney, J., and Chen, W. Non-cytotoxic, *in situ* gelable hydrogels composed of N-carboxyethyl chitosan and oxidized dextran. *Biomaterials* **29**, 3905, 2008.
31. Weng, L., Chen, X., and Chen, W. Rheological characterization of *in situ* crosslinkable hydrogels formulated from oxidized dextran and N-carboxyethyl chitosan. *Biomacromolecules* **8**, 1109, 2007.
32. Lewis, G. Nucleus pulposus replacement and regeneration/repair technologies: present status and future prospects. *J Biomed Mater Res A* **100**, 1702, 2012.
33. Costi, J.J., Freeman, B.J., and Elliott, D.M. Intervertebral disc properties: challenges for biodevices. *Expert Rev Med Devices* **8**, 357, 2011.
34. Maroudas, A., Stockwell, R.A., Nachemson, A., and Urban, J. Factors involved in the nutrition of the human lumbar intervertebral disc: cellularity and diffusion of glucose *in vitro*. *J Anat* **120**, 113, 1975.
35. Stoyanov, J.V., Gantenbein-Ritter, B., Bertolo, A., Aebli, N., Baur, M., Alini, M., *et al.* Role of hypoxia and growth and differentiation factor-5 on differentiation of human mesenchymal stem cells towards intervertebral nucleus pulposus-like cells. *Eur Cell Mater* **21**, 533, 2011.
36. Erickson, I.E., Huang, A.H., Chung, C., Li, R.T., Burdick, J.A., and Mauck, R.L. Differential maturation and structure-function relationships in mesenchymal stem cell- and chondrocyte-seeded hydrogels. *Tissue Eng* **15**, 1041, 2009.
37. Malhotra, N.R., Han, W.M., Beckstein, J., Cloyd, J., Chen, W., and Elliott, D.M. An injectable nucleus pulposus implant restores compressive range of motion in the ovine disc. *Spine (Phila Pa 1976)* **37**, E1099, 2012.
38. Hart, L.G., Deyo, R.A., and Cherkin, D.C. Physician office visits for low back pain. Frequency, clinical evaluation, and treatment patterns from a U.S. national survey. *Spine (Phila Pa 1976)* **20**, 11, 1995.
39. Bowles, R.D., Gebhard, H.H., Hartl, R., and Bonassar, L.J. Tissue-engineered intervertebral discs produce new matrix, maintain disc height, and restore biomechanical function to the rodent spine. *Proc Natl Acad Sci U S A* **108**, 13106, 2011.
40. Nerurkar, N.L., Sen, S., Huang, A.H., Elliott, D.M., and Mauck, R.L. Engineered disc-like angle-ply structures for intervertebral disc replacement. *Spine* **35**, 867, 2010.
41. Wuertz, K., Godburn, K., and Iatridis, J.C. MSC response to pH levels found in degenerating intervertebral discs. *Biochem Biophys Res Commun* **379**, 824, 2009.
42. Wuertz, K., Godburn, K., Neidlinger-Wilke, C., Urban, J., and Iatridis, J.C. Behavior of mesenchymal stem cells in the chemical microenvironment of the intervertebral disc. *Spine (Phila Pa 1976)* **33**, 1843, 2008.
43. Farrell, M.J., Comeau, E.S., and Mauck, R.L. Mesenchymal stem cells produce functional cartilage matrix in three-dimensional culture in regions of optimal nutrient supply. *Eur Cell Mater* **23**, 425, 2012.
44. Le Maitre, C.L., Hoyland, J.A., and Freemont, A.J. Catabolic cytokine expression in degenerate and herniated human intervertebral discs: IL-1beta and TNFalpha expression profile. *Arthritis Res Ther* **9**, R77, 2007.
45. Felka, T., Schafer, R., Schewe, B., Benz, K., and Aicher, W.K. Hypoxia reduces the inhibitory effect of IL-1beta on chondrogenic differentiation of FCS-free expanded MSC. *Osteoarthritis Cartilage* **17**, 1368, 2009.
46. Gorth, D.J., Mauck, R.L., Chiaro, J.A., Mohanraj, B., Hebel, N.M., and Dodge, G.R., *et al.* IL-1ra delivered from poly(lactic-co-glycolic acid) microspheres attenuates IL-1beta-mediated degradation of nucleus pulposus *in vitro*. *Arthritis Res Ther* **14**, R179, 2012.

Address correspondence to:  
Neil R. Malhotra, MD  
Department of Neurosurgery  
University of Pennsylvania  
3 Silverstein Pavilion  
3400 Spruce Street  
Philadelphia, PA 19104

E-mail: neil.malhotra@uphs.upenn.edu

Received: August 16, 2013

Accepted: January 6, 2014

Online Publication Date: March 19, 2014